Azhar Int J Pharm Med Sci 2022; Vol 2 (2): 9-20
Research article

Open Acces

Print ISSN: 2735-4598

Online ISSN: 2735-4601

Design, synthesis and antiproliferative evaluation of novel Pyrazolo-pyrimidine derivatives with expected Cyclin-dependent kinase 2 inhibitory effect

Amel S. Younes [1], Taghreed Z. Shawer [1*] and Hend M.A. El-Sehrawi1[1]

[1] Department of Pharmaceutical Medicinal Chemistry and Drug Design, Faculty of Pharmacy (girls), Al-Azhar University, Nasr City, Cairo, Egypt

***** Correspondence: taghreedshawer@azhar.edu.eg

Article history: Received: 26-05-2021 **Revised:01-09-2021** **Accepted: 03-10-2021**

Abstract:

A series of novel pyrazolopyrimidines **2-11** have been designed and synthesized. Depending on the screening program of NCI, **2-11** have been estimated in vitro for their anti-proliferative properties on 60 cell line subpanels. Among them, compounds **6** and **11** displayed excellent antiproliferative effects against glioma cell line (SF-539) with GI values of 85.85% and 63.65%, respectively. Therefore, the IC_{50} values for compounds **6** and **11** against the SF-539 cell line were obtained with the best results, using Roscovitine as a positive control. Compound **6** showed the best inhibitory activity with IC_{50} value of 11.1 µM, representing 1.5-folds the potency of Roscovitine, while compound **11** exhibited 71% the inhibitory activity of the reference used. Enzymatic inhibition studies on compound **6** show that it has activity on cyclin-dependent kinase 2 (CDK2/cyclinA) with IC_{50} equal 0.76 µM, compared to Roscovitine (IC_{50} = 0.44 µM). Compound **6** was tested for toxicity against normal human lung cell line (WI-38), and it possessed no toxicity against it. Its IC_{50} value was found to be 66.20 µM. A docking investigation was done to disclose interactions of compounds **6** and **11** in the CDK2 kinase's active site. Computational ADME analysis was achieved to ensure that, compounds **6** and **11** have appropriate pharmacokinetic and drug-likeness characteristics.

Keywords: pyrazolopyrimidine; cyclin-dependent kinase 2; ADME analysis.

1. Introduction

Brain malignancy treatment is among the most challenges in oncology. The primary brain tumors are thought to be derived from glial cells or their progenitors and are generally classified as gliomas [1,2]. Glioblastoma multiforme (GBM) is a malignant form of glioma characterized by widespread proliferation and metastasis [3]. It remains one of the most aggressive solid tumors. It is highly resistant to conventional chemotherapy, can achieve high recurrence rates in affected individuals, and has an average life expectancy of less than 14 months [4]. Although the standard care programs including surgery, radiation therapy, and chemotherapy can provide successful initial treatment, disease recurrence is predictable and always fatal in most cases of GBM. Therefore, improving the therapy for GBM either by novel therapeutics or by supplementing new strategies is required [4-6]. The research for novel druggable molecular targets, as well as the development of their modulators as new medications for cancer treatment, has become an important medical goal. Protein kinases have emerged as an important therapeutic goal, as the variety of kinase inhibitors being tested in medical testing is fast growing [7]. CDKs are a class of serine-threonine kinases composed of regulatory cyclin and catalytic kinase subunits. They contain a family that is classified into two categories depending on their functions in cell cycle progression and transcriptional control [7,8]. In addition, compared with normal brain cells, the expression of CDK2 in GBM tumors is dramatically amplified [8]. Hence, CDKs are thought to be a good target for anticancer treatments.

Pyrazole and fused pyrazole derivatives have shown a wide range of medical applications and have

Cite this article: Younes A., Shawer T.and El-Sehrawi1 H. Design, Synthesis and Antiproliferative Evaluation of Novel Pyrazolo-pyrimidine Derivatives with Expected Cyclin-dependent kinase 2 Inhibitory Effect**.** Azhar International Journal of Pharmaceutical and Medical Sciences, 2022; 2(2):9-20. doi: 10.21608/AIJPMS.2022.77353.1075

DOI : 10.21608/AIJPMS.2022.77353.1075 https://aijpms.journals.ekb.eg/

received special consideration in the field of cancer treatment [9,10]. Pyrazolopyrimidine is found to have diverse activities, including antimicrobial, anti-inflammatory and anticancer, in addition to its activities on central nervous system [7]. Recent studies have shown that pyrazolopyrimidine derivatives exhibit significant antiproliferative effects against different tumor cell lines by inhibiting the CDK2 enzyme [7,11,12].

Roscovitine **1** and Olomoucine **2** are well-known purine analogues, they are potent cdk inhibitors (IC_{50} for cdk1/cdk2 equal 0.7 µM and 7 µM, respectively) [13]. Compounds **3** and **4** revealed significant enzymatic inhibitory activity against CDK2 with IC_{50} values of 5.1 and 6.8 µM, respectively[7,12]. Roscovitine **1** has been utilized in clinical studies for a variety of malignancies. It doesn't only inhibit CDKs implicated in the cell cycle (2, 7, 8, and 9), but also inhibits CDK5, that is involved in cell migration. This dual effect make Roscovitine a promising therapeutic candidate for GMB treatment [14]. Several human cancer cell lines, including ovarian, pancreatic, kidney, breast, hepatic, pituitary, neuroblastoma and colon are inhibited by Roscovitine [15-21]. It has been investigated in phase I and II clinical studies in a variety of human cancers, both as a monotherapy and combination therapy [22]. **Figure 1** depicts some reported anticancer agents as CDK inhibitors [7,12,13].

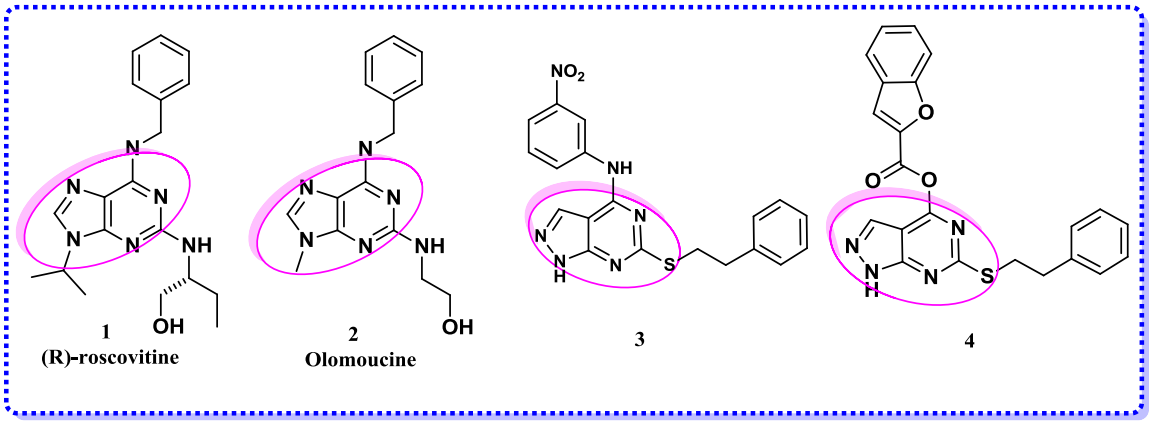

Figure 1. Structures reported as CDK inhibitors.

Based on the above data, our aim was to synthesize a series of novel pyrazolopyrimidines with a design strategy based on Roscovitine, as shown in **Figure 2**, and then study their antiproliferative activity and CDK2 inhibitory effect. The optimization of the targeted compounds depends on the following approaches: bioisosteric replacement, simplification of amino-butanol, substituent variation of isopropyl group and chain contraction.

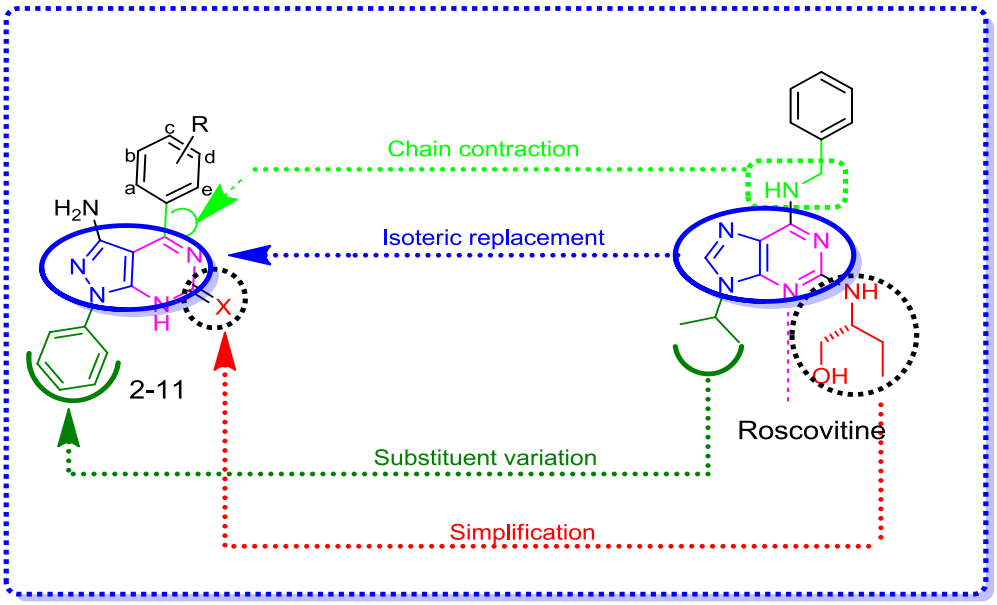

Figure 2. Structure-based design of targeted compounds via modification of Roscovitine.

2. Materials and Methods

2.1. Chemistry

The open capillary tube method was used to measure melting points with instrument, namely the Stuart SMP3 Melting. The Regional Center for Mycology and Biotechnology at Al-Azhar University conducted elemental analysis. At the Armed Forces Laboratories, on a Bruker ATR/FTIR Spectrophotometer, IR spectra were recorded using KBr [**IR (KBr) (cm^{-1})**]. Both ^{1}H NMR [(**400 MHZ, DMSO-d_6) δ (ppm**)] and ^{13}CNMR[(**DMSO-d_6) δ(ppm**)] spectra were acquired using a Varian Gemini 300 MHz Spectrophotometer. It has been used to analyze the spectra at 300 MHz in DMSO d6 (deuterated dimethyl sulfoxide). Chemical shifts were expressed in d units and were related to that of the solvents. D_2O was used to conduct proton magnetic resonance intended for amine and hydroxy protons. Mass spectra (***m/z***) were obtained at 70 eV by means of a Shimadzu Gas Chromatograph Mass Spectrometer-Qp 2010 plus at Al-Azhar University. Thin layer chromatography was used to monitor all the reactions, which were carried out on silica gel and observed using lamp of UV. compound **1** was prepared as reported [23].

2.1.1. General Synthetic procedure of 3-amino-1-phenyl-4-(phenyl/substitutedphenyl)-4,5-dihydro-1H-pyrazolo[3,4-d] pyrimidin-6(3aH)-ones (2-6)

A solution of compound **1** (1.75g, 0.01 mol), urea (0.60 g, 0.01mol) and 0.01 mol of appropriate aldehyde (viz. benzaldehyde, 4-chloro benzaldehyde, 4-methoxy benzaldehyde, 2,4-di chloro benzaldehyde or 2,5-dimethoxy benzaldehyde), in 15mL of absolute EtOH, with three drops of triethylamine, was allowed to react for 6-10 hrs. The obtained product was filtered in and crystallized from EtOH after cooling.

2.1.1.1. 3-Amino-1,4-diphenyl-4,5-dihydro-1H-pyrazolo[3,4-d] pyrimidin-6(3aH)-one (2) IR: 3366 (NH), 3253 (br., NH_2), 1692 (C=O), 1626 (C=N). ^{1}H-NMR: 4.41 (d, 1H, CH-pyrimidine), 4.95 (d, 1H, CH-pyrimidine), 7.02-8.11 (m, 10H, Ar-H_{a-e}+ Ph-H_{2-6}), 9.74 (s, 3H, NH_2+NH). MS: 305 (M^+, 4.74%), 263 (100%). ^{13}C-NMR: 44.43, 56.96, 118.01, 118.69, 124.64, 127.56, 128.22, 128.58, 134.63, 157.51, 158.99, 167.48.

2.1.1.2. 3-Amino-4-(4-chlorophenyl)-1-phenyl-4,5-dihydro-1H-pyrazolo [3,4-d] pyrimidin-6(3aH)-one (3) IR: 3443, 3341(NH_2), 3209 (NH), 1673 (CO), 1627 (C=N). ^{1}H-NMR: 4.47 (d, 1H, CH-pyrimidine), 4.87 (d, 1H, CH-pyrimidine), 5.42 (s, 2H, NH_2), 6.10 (s, 1H, NH), 7.04-7.95 (m, 9H, Ar-H_{a-e}+Ph-H_{2-6}). MS: 339 (M^+, 37.42%), 341(M^++2, 27.49%), 299 (100%).

2.1.1.3. 3-Amino-4-(4-methoxyphenyl)-1-phenyl-4,5-dihydro-1H-pyrazolo[3,4-d]pyrimidin-6(3aH)-one (4) IR: 3308, 3224, (NH+NH_2), 1687 (CO), 1631 (C=N). ^{1}H-NMR: 3.74 (s, 1H, OCH_3), 4.27 (d, 1H, CH-pyrimidine), 4.85(d, 1H, CH-pyrimidine), 6.77-7.44 (m, 9H, Ar-H_{a-e} + Ph-H_{2-6}), 7.68 (s, 1H, NH), 7.99 (s, 2H, NH_2). MS: 335 (M^+, 24.86%), 76 (100%). ^{13}C-NMR: 44.55, 54.46, 55.53, 113.56, 118.66, 124.34, 126.53, 128.27, 129.39, 130.72, 138.13, 158.91, 159.74, 167.20.

2.1.1.4. 3-Amino-4-(2,4-dichlorophenyl)-1-phenyl-4,5-dihydro-1H-pyrazolo[3,4-d]pyrimidin-6(3aH)-one (5) IR: 3447 (NH), 3333 (br., NH_2), 1703 (CO), 1626 (C=N). ^{1}H-NMR: 4.47 (d, 1H, CH-pyrimidine), 4.70 (d, 1H, CH-pyrimidine), 5.46 (s, 2H, NH_2), 7.02-7.98 (m, 8H, Ar-$H_{a,b,d}$+ Ph-H_{2-6}), 8.17 (s, 1H, NH). MS: 373 (M^+, 35.04%), 375 (M^++ 2, 5.75%), 134 (100%).

2.1.1.5. 3-Amino-4-(2,5-dimethoxyphenyl)-1-phenyl-4,5-dihydro-1H-pyrazolo[3,4-d] pyrimidin-6(3aH)-one (6) IR: 3325, 3276 (NH+ NH_2), 1698 (CO), 1646 (C=N). ^{1}H-NMR: 3.62, 3.72 (2s, 6H, 2OCH_3), 4.43 (d, 1H, CH-pyrimidine), 5.40 (d, 1H, CH-pyrimidine) , 6.85-7.56 (m, 6H, Ar-$H_{a,c,d}$+ Ph-$H_{3,4,5}$), 7.56 (d, 2H, Ph-$H_{2,6}$), 7.75 (s, 1H, NH), 8.10 (s, 2H, NH_2). MS: 365 (M^+, 59.13%), 222 (100%). ^{13}C-NMR: 52.56, 55.13, 56.37, 56.47, 112.59, 112.74, 113.39, 118.30, 124.19, 128.91, 138.27, 151.53, 152.56, 152.86, 159.35, 165.96, 167.07.

2.1.2. General Synthetic procedure of 3-amino-1-phenyl-4-(phenyl/substituted phenyl) -1H-pyrazolo [3,4-d] pyrimidine-6(7H)-thiones (7-11)

We added 0.01 mol of the suitable aldehyde (namely benzaldehyde, 4-chloro benzaldehyde, 4-methoxy benzaldehyde, 2,4-di chloro benzaldehyde or 2,5-dimethoxy benzaldehyde) and thiourea (0.76 g, 0.01 mol) to a solution of starting material **1** (1.75 g, 0.01 mol), in dioxan (20 mL) with three droplets of triethylamine. The entire mixture of reaction was heated at reflux for 7-10 hours. Filtration was used to collect the powdered precipitate, and then it crystallized from DMF.

2.1.2.1. 3-Amino-1,4-diphenyl-1H-pyrazolo[3,4-d] pyrimidine-6(7H)-thione(7) IR: 3424 (br., NH_2+NH) , 1599 (C=N). ^{1}H-NMR: 7.26-7.87 (m, 10H, Ar-H_{a-e}+ Ph-H_{2-6}). MS: 319 (M^+, 72.61%), 235 (100%).

2.1.2.2. *3-Amino-4-(4-chlorophenyl)-1-phenyl-1H-pyrazolo[3,4-d]pyrimidine-6(7H)-thione(8)* IR: 3422 (br., NH_2), 3200 (NH), 1572 (C=N). ^{1}H-NMR: 7.30-7.38 (m, 3H, Ar-$H_{b,d}$+ Ph-H_4), 7.55 (d, 2H, Ar-$H_{a,e}$), 7.85-7.98 (m, 4H, Ph-$H_{2,3,5,6}$). MS: 353 (M^+, 58.32%), 355 (M^++2 7.70%), 147 (100%).

2.1.2.3. 3-Amino-4-(4-methoxyphenyl)-1-phenyl-1H -pyrazolo[3,4-d] pyrimidine-6(7H)-thione (9) IR: 3416, 3386 (NH_2), 3261 (NH), 1609 (C=N). ^{1}H-NMR: 3.77(s, 3H, OCH_3), 6.95-7.42 (m, 7H, Ar-H_{a-e} + Ph-$H_{3,4,5}$), 7.91 (d, 2H, Ph-$H_{2,6}$), 7.95 (S, 3H, NH_2+NH). MS: 349 (M^+, 33.03%), 272 (100%).

2.1.2.4. 3-Amino-4-(2,4-dichlorophenyl)-1-phenyl-1H-pyrazolo[3,4-d]pyrimidine-6(7H)-thione (10) IR (KBr) (cm^{-1}): 3365, 3274 (NH_2), 3170 (NH), 1608 (C=N). ^{1}H-NMR: 6.70(S, 2H, NH_2), 6.99-7.77 (m, 6H, Ar-$H_{a,b,d}$+ Ph-$H_{3,4,5}$), 8.00 (d, 2H, Ph-$H_{2,6}$), 8.40 (S, 1H, NH). MS: 387 (M^+, 13.44%), 389 (M^++2, 3.96%), 333 (100%). ^{13}C-NMR: 46.15, 66.82, 118.06, 119.66, 127.16, 129.07, 131.46, 132.81, 135.48, 138.74, 158.03, 160.98, 169.80, 184.26.

2.1.2.5. 3-Amino-4-(2,5-dimethoxyphenyl)-1-phenyl-4,5-dihydro-1H-pyrazolo[3,4-d] pyrimidine-6(7H)-thione (11) IR: 3425, (br., NH_2), 3213 (NH), 1654 (C=N). ^{1}H-NMR: 3.70, 3.78 (2s, 6H, 2OCH_3), 4,44 (d, 1H, CH-pyrimidine), 5.42 (d, 1H, CH-pyrimidine) , 6.51 (S, 1H, NH), 6.70-7.76 (m, 8H, Ar-$H_{a,c,d}$+Ph-H_{2-6}), 8.11 (S, 2H, NH_2). MS: 379 (M^+, 29.32%), 77 (100%). ^{13}C-NMR: 46.20, 52.58, 56.47, 56.8, 111.93, 112.58, 113.13, 118.25, 123.59, 129.33, 138.09, 151.13, 152.21, 152.57, 159.35, 167.07, 184.27.

Table 1. Physical properties and elemental analysis of the newly synthesized compounds **2-11**

Comp.no.	Yield (%)	M.P (ºC)	Mol. Formula (M. Wt)	Elemental analysis [%] Calcd.(Found)		
				C	H	N
2	**34**	**250-252**	**$C_{17}H_{15}N_5O$ (305.13)**	**66.87(66.88)**	**4.95(4.93)**	**22.94(22.95)**
3	**37**	**148-150**	**$C_{17}H_{14}ClN_5O$ (339.09)**	**60.09(60.10)**	**4.15(4.17)**	**20.61(20.60)**
4	**37**	**255-257**	**$C_{18}H_{17}N_5O_2$ (335.14)**	**64.47(64.45)**	**5.11(5.10)**	**20.88(20.86)**
5	**37**	**153-155**	**$C_{17}H_{13}Cl_2N_5O$ (373.05)**	**54.56(54.55)**	**3.50(3.51)**	**18.71(18.71)**
6	**33**	**228-230**	**$C_{19}H_{19}N_5O_3$(365.15)**	**62.46(62.44)**	**5.24(5.25)**	**19.17(19.16)**
7	**42**	**393-395**	**$C_{17}H_{13}N_5S$ (319.09)**	**63.93(63.92)**	**4.10(4.09)**	**21.93(21.95)**
8	**41**	**298-300**	**$C_{17}H_{12}ClN_5S$ (353.05)**	**57.71(57.70)**	**3.42(3.42)**	**19.79(19.78)**
9	**38**	**293-295**	**$C_{18}H_{15}N_5OS$ (349.10)**	**61.87(61.88)**	**4.33(4.31)**	**20.04(20.05)**
10	**38**	**173-175**	**$C_{17}H_{11}Cl_2N_5S$ (387.01)**	**52.59(52.60)**	**2.86(2.85)**	**18.04(18.02)**
11	**39**	**223-225**	**$C_{19}H_{17}N_5O_2S$ (379.11)**	**60.14(60.15)**	**4.52(4.50)**	**18.46(18.45)**

2.2. Biological assessment

2.2.1. In-vitro Cytotoxic efficacy of pyrazolo-pyrimidines (NCI, USA)

The NCI anticancer screening approach is detailed at (http://www.dtp.nci.nih.gov) [24]. For more information, *see* **supplementary file**.

2.2.2. MTT cytotoxicity assay of target compounds 6 and 11 against SF-539 cancer cell line [25].

In order to evaluate the tested compound's IC_{50}, the MTT test was employed. In **Supplementary file**, the MTT method was described in detail.

2.2.3. In vitro cyclin dependent kinase2 inhibitory activity:

Using the ADP-GloTM Kinase Assay, compound **6** was evaluated *in vitro* for inhibition of CDK2 tyrosine kinase (Promega, Catalogue No. V3831) [26]. *See* **Supplementary File** for more details

2.3. In silico studies

2.3.1. In silico physicochemical and ADME parameters calculation

Physicochemical properties, ADME characteristics, pharmacokinetic features, hydrophobicity, and medicinal chemistry friendliness were calculated using SwissADME website [27]. See **Supplementary file** for more data.

2.3.2. Molecular modeling:

The PDB (ID: 2A4L) [7] (http://www.pdb.org) was utilized to obtain crystallographic structures of CDK2 that were used as docking simulation targets. During the docking investigation, MOE software was used to evaluate the proposed compounds' free energies and binding modes against CDK2. In **Supplementary file**, the docking process is clearly described

3. RESULTS

3.1. Chemistry

The targeted compounds **2-11** were prepared following the procedures indicated in Schemes 1 and 2. Pyrazolopyrimidines **2-6** were prepared *via* one-pot reaction of compound **1**, appropriate aromatic aldehyde and urea, in ethanol, using triethylamine as catalyst [28]. Compounds **7-11** were synthesized via multi-compartment reaction of **1**, appropriate aromatic aldehyde and thiourea, in dioxane, using trimethylamine as catalyst [10].

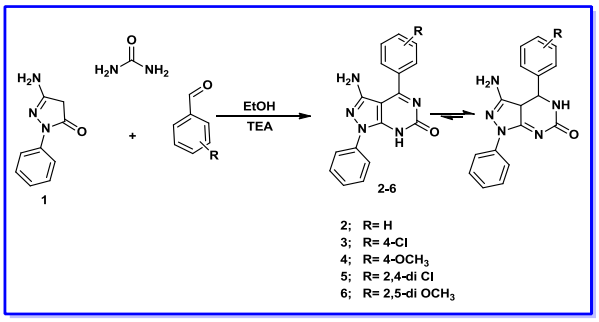

Sheme1:Route for the synthesis of compounds **2-6.**

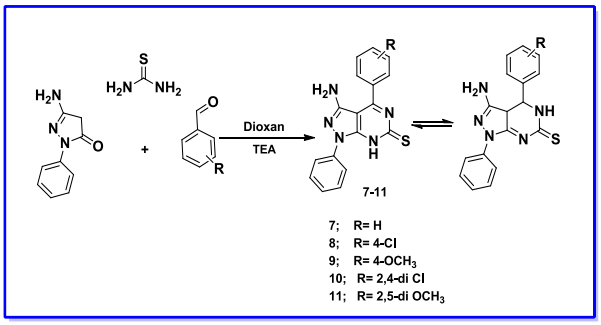

Scheme 2: Route for the synthesis of compounds **7-11.**

3.2. Biological assessment

3.2.1. Preliminary In-Vitro Antitumor Screening:

The NCI, Germantown, MD, USA, examined the produced compounds on 60 cell line subpanels, including prostate, colon, breast, CNS, ovarian, leukemia, non-small cell lung, melanoma and renal malignancies, as part of the Development Therapeutic Program (DTP).

The compounds were tested in a single dosage at concentration of 10 µM. The data are expressed as percentage of the treated cells' growth inhibition (GI%). The results of the assay listed in **Table 2** suggested that compounds **6** and **11** revealed the highest activity against SNB-539, CNS cancer subpanel, with GI values of **85.85** and **63.65%**, respectively.

3.2.2. In-vitro IC_{50} study for compounds 6 and 11:

The IC_{50} values of the maximum potent analogues **6** and **11**, in the NCI assay, have been assessed against the tumor cell line, namely SF-539, using Roscovitine as a positive control (**Table 3**).

3.2.3. In-vitro CDK2/cyclinA inhibitory activity:

Compound **6**, possessing the highest activity, was chosen to investigate the mechanism of action through estimation of its inhibitory impact against CDK2. In comparison to the reference (IC_{50} =0.44 M), the evaluated component **6** demonstrated inhibitory activity with an IC_{50} of 0.76 M. (**Table 4**).

3.2.4. Cytotoxicity towards non-tumorigenic cells for compound 6:

To explore the selectivity towards cancer cells, compound **6** was assessed for cytotoxicity against the non-tumorigenic lung fibroblast (WI38), via the MTT assay. The obtained IC_{50}s are presented in **Table 4**.

3.3. In silico analysis

3.3.1. ADME study and pharmacokinetic properties prediction for compounds 6 and 11:

Using computational devices to identify new drug candidates can help to decrease the number of experimental trials and boost the rate of success. As a result, we used the SwissADME (www. Swissadme. ch/) online tool to apply Lipinski's and Veber's rules for drug similarity as a key screening step evaluating oral bioavailability and synthetic availability [37]. The calculation results are shown in **Table 5.**

3.3.2. Molecular docking study for compounds 6 and 11:

Docking analysis has been done to investigate interactions of the most powerful compounds **6** and **11** with crucial amino acids in the CDK2 enzyme's active site in order to explain their potential inhibitory activity. Molecular Operating Environment (MOE ®)2008.10 was utilized to evaluate techniques of docking and to duplicate the predicted configuration of R-roscovitine in CDK2 [7]. R-roscovitine pose was found to have identical interactions as documented (**Figure 4**). The docking experimental data of compounds **6** and **11** showed that they interacted successfully with the active binding region (**Figure 5 &6**). **Figure 3** depicts 3D structure overlying of **Roscovitine**, **6** and **11** within CDK2 kinase active site.

Table 2. Growth inhibition percent of the tested compounds against 60 different cell lines.

Comp.no. (NCI-No.)	Panel: subpanel cell line (growth inhibition percent)
2 (D-823706 / 1)	**Leukemia:** MOLT-4 (12.87) **Non-Small Cell Lung Cancer:** EKVX (17.87), NCI-H522(13.16) **CNS Cancer:** U251(14.90) **Melanoma:** M14(11.22), SK-MEL-2(10.57), UACC-257(17.57) **Renal Cancer:** A498(16.00), CAKI-1(17.75), SN12C (11.33), TK-10(14.96), UO-31(**23.09**), PC-3 (15.57) **Breast Cancer:** MCF7(15.01), T-47D (11.26)
3 (D-823710/ 1)	**Leukemia:** CCRF-CEM (15.34), K-562(17.24), MOLT-4(11.46), SR (29.71) **Non-Small Cell Lung Cancer:** A549/ATCC (**30.67**), EKVX (14.53), HOP-92 (26.47), NCI-H226(11.70), NCI-H460 (20.30), NCI-H522 (23.90) **Colon Cancer:** HCT-116 (12.07), SW-620 (13.82) **CNS Cancer:** SF-268(11.45), SNB-19(12.14), SNB-75 (13.46) **Melanoma:** SK-MEL-5 (23.73), UACC-62 (**28.92**) **Ovarian Cancer:** IGROV1(13.11), OVCAR-4(12.55) **Renal Cancer:** A498(14.12), ACHN (10.8), CAKI-1(19.18), SN12C (18.12), UO-31(**36.38**) **Prostate Cancer:** PC-3(15.15) **Breast Cancer:** MCF7(19.52), MDA-MB-231/ ATCC (11.65), T-47D (14.21)
4 (D-823714 /1)	**Leukemia:** SR (**27.22**) **Non-Small Cell Lung Cancer:** A549/ATCC (**27.71**), EKVX (13.93), NCI-H522 (11.31) **Melanoma:** UACC-6212.40 **Renal Cancer:** CAKI-1(17.77), TK-10 (11.24), UO-31(**25.83**) **Breast Cancer:** T-47D (10.08)
5 (D-823709 /1)	**Non-Small Cell Lung Cancer:** A549/ATCC (11.40), HOP-92(18.36) **CNS Cancer:** SNB-75(15.88), U251(15.31) **Melanoma:** UACC-62(19.47) **Ovarian Cancer:** IGROV1(17.37) **Renal Cancer:** CAKI-1 (15.03), SN12C (15.47), UO-31(31.59) **Prostate Cancer:** PC-3(14.62) **Breast Cancer:** T-47D (19.22)
6 (D-823712/1)	**Leukemia:** HL-60(TB) 28.04, K-562(16.06) **Colon Cancer:** HT29(19.84) **CNS Cancer: SF-539** (**85.85**), SNB-19 (11.78) **Melanoma:** MALME-3M (15.10) **Renal Cancer:** UO-31 (14.64)
7 (D-823705/1)	**Non-Small Cell Lung Cancer:** EKVX (13.34) **Ovarian Cancer:** IGROV1(10.21) **Renal Cancer:** UO-31 (**25.18**)
8 (D-823707/1)	**Renal Cancer:** UO-31(23.47)
9 (D-823713/1)	**Renal Cancer:** UO-31(24.65)
10(D-823708/1)	**Leukemia:** MOLT-4 (15.13), SR (10.88) **Non-Small Cell Lung Cancer:** EKVX (27.11), HOP-62(12.64), HOP-92 (**26.54**), NCI-H226 (13.93) **CNS Cancer:** SNB-19(11.53), SNB-75 (26.75), U251(11.27) **Melanoma:** UACC-257(21.32) **Renal Cancer:** CAKI-1(24.38), SN12C (10.79), UO-31(**34.99**) **Prostate Cancer:** PC-3 (15.79) **Breast Cancer:** MCF7(11.75), MDA-MB-231/ATCC (18.60), T-47D (14.43)
11(D-823711/1)	**Leukemia:** HL-60(TB) (20.89), K-562 (12.27), SR (15.21) **CNS Cancer:** SF-539 (**63.65**) **Melanoma:** UACC-62 (12.66) **Renal Cancer:** CAKI-1(10.86), UO-31(**24.75**) **Breast Cancer:** MCF7 (12.12)

Only GI% higher than 10% are shown.

Table 3: IC_{50} values of compounds **6** and **11** against the most sensitive cell line.

Cpd. No.	SF-539 (µM)[a]
6	**11.1±0.63**
11	**24.2±1.38**
Roscovitine	**17.3±0.99**

[a]IC_{50} values are the mean ± S.D. of three separate experiments.

Table 4: CDK2 Inhibitory activity and cytotoxicity against normal cell WI-38 for compound **6**.

Cpd. No.	CDK2 (µM)	WI38(µM)
6	**0.76±0.04**	**66.20±4.12**
Roscovitine	**0.44±0.01**	**54.48±2.72**

Table 5: Physicochemical properties based on Lipinski, Veber rules and pharmacokinetic properties for compounds **6** and **11** for assessment of the drug likeness

Properties	6	11	Roscovitine
MW	**365.3**	**365.3**	**354.4**
HBD	**2**	**2**	**3**
HBA	**5**	**5**	**4**
MLOGP	**2.5**	**2.5**	**1.61**
R. bonds	**4**	**4**	**8**
TPSA	**101.5**	**101.5**	**87.8**
% ABS	**73.96**	**73.96**	**78.67**
Lipinski´s Violations	**0**	**0**	**0**
VeberViolations	**0**	**0**	**0**
GI Absorption	**High**	**High**	**High**
Bioavailability Score	**0.55**	**0.55**	**0.55**
***PAINS Alerts**	**0**	**0**	**0**
Synthetic Accessibility	**4.46**	**4.46**	**3.58**

*PAINS Alerts were performed by SwissADME PAINS-Remover, free online servers

4. Discussion

4.1. Chemistry

As mentioned above, compounds **2-6** were produced following the processes indicated in Schemes 1. The isolated compounds' structures were confirmed according to their elemental analysis and spectrum data. The appearance of two doublet signals at the range of δ (4.27-5.40) ppm, assigned for two CH-pyrimidines, appeared in **^{1}H-NMR** spectra of compounds **2-6**, as well as an increase in the number of aromatic protons which confirmed their strucure. As an example of this series, Compound **4's IR** spectrum revealed absorption bands at 3308, 3224 and 1687 cm^{-1} attributable to NH, NH_2 and C=O groups, respectively. Compound **4's ^{1}H-NMR** spectrum indicated a single peak at δ 3.74 ppm corresponding to OCH_3 protons. Additional peaks were observed at δ 7.68 and 7.99 representing the exchangeable NH and NH_2 protons, along with an increase of four aromatic protons. **^{13}C-NMR** spectrum of **4** exhibited signals at 44.55, 54.46 and 55.53 ppm related to two CH-pyrimidine, and OCH_3 carbons, in addition to a signal at 167.20 ppm representing CO carbon. Compound **4's** mass spectrum revealed a molecular ion peak at m/z 335.

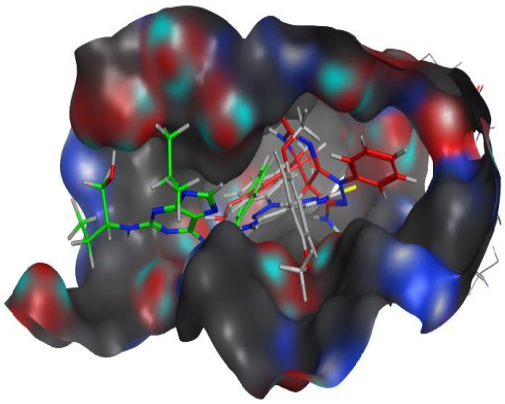

Figure 3. Overlay docking alignment of Roscovitine (green), **6** (red) **11** (grey) compounds docked into in the active site of CDK2 (PDB code: 2A4L).

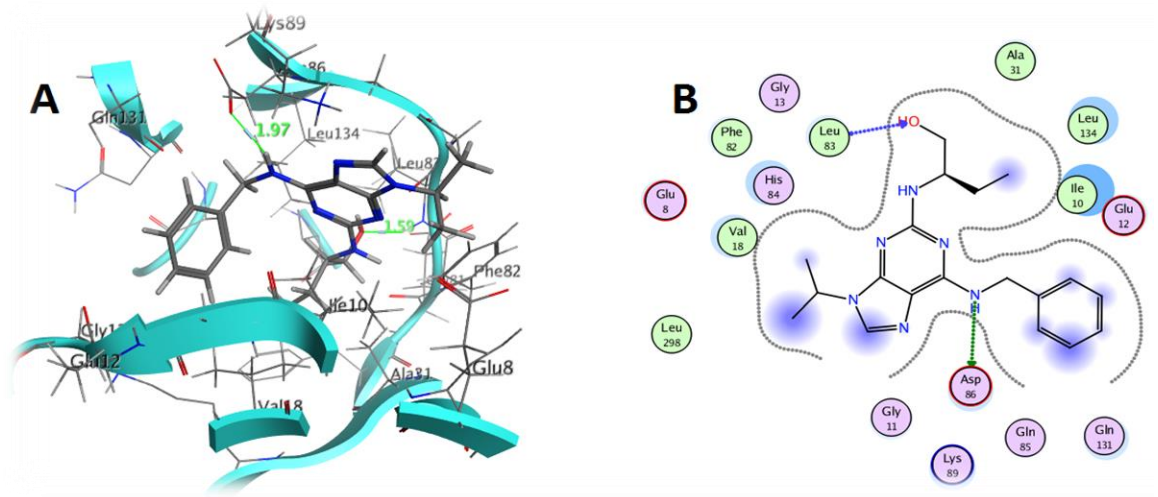

Figure 4. The proposed binding mode of **Roscovitine** docked in the active site of CDK2; **A** and **B** showing 3D and 2D ligand-receptor interactions (hydrogen bonds are illustrated as arrows; C atoms are colored gray, N blue and O red).

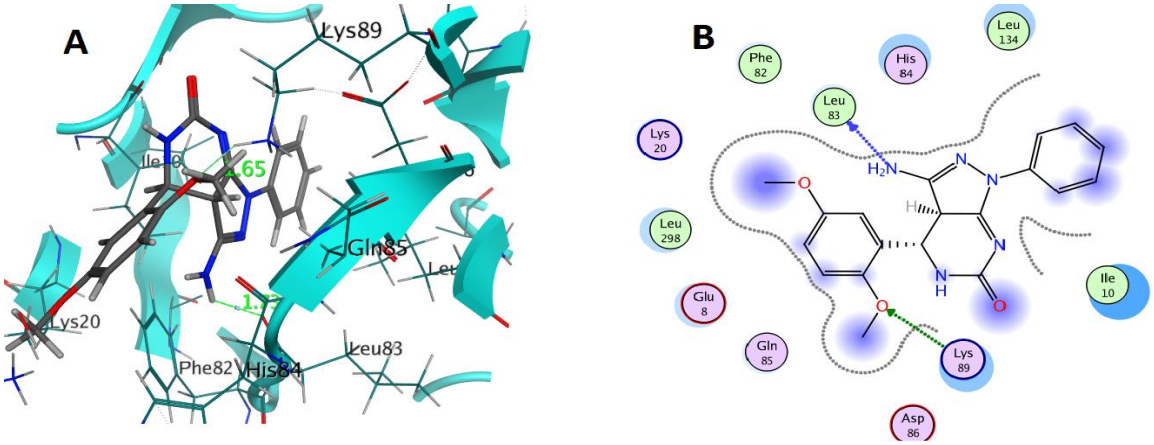

Figure 5. The proposed binding mode of **6** docked in the active site of CDK2; **A** and **B** showing 3D and 2D ligand-receptor interactions (hydrogen bonds are illustrated as arrows; C atoms are colored gray, N blue and O red).

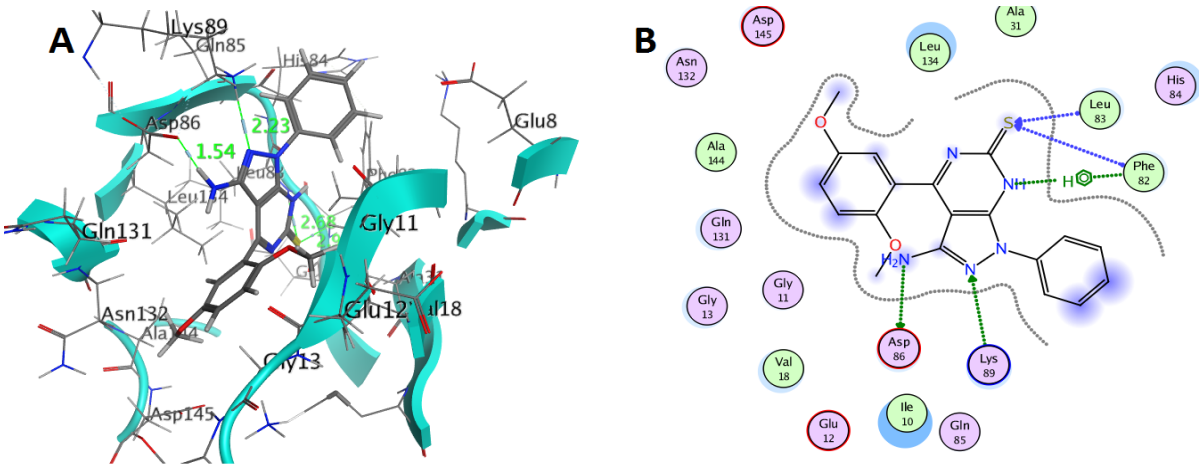

Figure 6. The proposed binding mode of **11** docked in the active site of CDK2; **A** and **B** showing 3D and 2D ligand-receptor interactions (hydrogen bonds are illustrated as arrows; C atoms are colored gray, N blue and O red).

The production of **7-11**, as shown in **Scheme 2**. Analytical and spectroscopic measurements confirmed their structures. All compounds in **IR** spectra exhibited a newly band at the range of (3216-3170) cm^{-1} attributed to the NH group, along with the disappearance of the carbonyl band of the parent compound. **^{1}H-NMR** spectra for compounds **7-11** shared a common feature, which is the disappearance of a single peak at δ 3.82 ppm, corresponding to CH_2 of the parent compound, as well as an increase in the number of aromatic protons. Strong bands related to NH_2 and NH groups were disclosed in the **IR** spectrum of compound **9** at 3416, 3386 and 3261 cm^{-1}, as well as the non-appearance of the CO band of the parent compound. Further, a single peak at 3.77 ppm in the **^{1}H-NMR** spectrum indicated OCH_3 protons. Additional peaks were observed at δ 7.95 representing exchangeable NH_2 and NH protons. Additionally, the spectrum of **^{13}C-NMR** for compound **11** showed peaks at 46.20 and 52.58 for the pyrimidine carbons, plus three peaks at 56.47, 56.88 and 184.27 corresponding to two OCH_3 and C=S carbons, respectively.

4.2. Biological assessment

4.2.1. In-Vitro Screening for cytotoxicity

According to the results shown in **Table 2**, pyrazolopyrimidine **6** and **11** exhibited the greatest effect against SNB-539 with GI values of **85.85** and **63.65%**, respectively.

Exploring the obtained percentage of GI values, compound **3** exhibited moderate anti-proliferative with wide range activity against Leukemia (SR), Lung Cancer (HOP-92 and A549/ATCC), Renal cancer subpanels(UO-31) and Melanoma (UACC-62) with GI values in the range of 36.38-26.47%. In contrast, anti-proliferative activity against these cell lines was decreased or abolished when treated with compound **8.**

Compound **4** showed GI values of 27.22 and 27.71% against Leukemia subpanels (SR) and Lung Cancer (A549/ATCCcell line), respectively. By replacement of oxo-group with thione-group in compound **9**, the anti-proliferative activity was diminished.

Renal cancer subpanels (UO-31) was inhibited by compounds **4**, **5**, **7** and **10** with GI values in the range of 34.99-25.18%. In addition, Leukemia subpanels (HL-60) was inhibited by compounds **6** and **11** with GI values 28.04 and 20.89%, while **10** displayed growth inhibitory activity against Lung Cancer (EKVX and HOP-92) with GI values of 26.54 % and 27.11%, respectively.

Based on the above results, the structure-activity correlation of the newly synthesized compounds can be summarized as follows (**Figure 7**):

Fusion of oxo-pyrimidine moiety with pyrazole improves anti-proliferative activity as in compounds **2-6**, whereas the anti-proliferative activity was decreased in the corresponding thione analogues as in compounds **7-11**.

The presence of 2,5-dimethoxy substituent on the phenyl group in pyrazolo[3,4-d] pyrimidine moiety improved both activity and selectivity as compounds **6** and **11** that demonstrated potent antitumor activity against malignant CNS cell line (SNB-539).

4.2.2. In-vitro IC_{50} study for compounds 6 and 11:

In-vitro study of the most powerful analogues **6** and **11** against human glioma cell line (SF-539) disclosed that compound **6** (IC_{50} = 11.1µM) gave 1.5-folds the potency of Roscovitine (IC_{50} = 17.3µM), while **11** exhibited 71% the inhibitory activity of the reference used (IC_{50}, 24.2µg/mL vs 17.3µg/mL) (**Table 3**).

4.2.3. In-vitro CDK2/cyclin A inhibitory activity:

CDK2 has been linked to cancer cell hyper-proliferation and is considered to be a therapeutic target in the treatment of cancer [8]. CDK2 encourages proliferation, promotes radio resistance in GBM, and it may be a potential therapeutic target for GBM [8]. The tested compound **6** showed 57% of inhibitory activity with IC_{50} of 0.76 µM, in comparison to the reference (Roscovitine IC_{50} =0.44 µM) (**Table 4**).

4.2.4. Cytotoxicity towards non-tumorigenic cells for compound 6:

Compound **6**'s cytotoxicity against WI38 was tested using the MTT assay to see if it was selective for cancer cells (**Table 4**). It exhibited selective cytotoxicity against cancer cells and less toxicity towards normal cell line (IC_{50}= 66.20 µM) as compared with Roscovitine (IC_{50}; 54.48µM).

4.3. In silico analysis

4.3.1. ADME study and pharmacokinetic properties prediction for compounds 6 and 11:

The calculation results shown in **Table 5** illustrated that, the most active compounds **6** and **11**, follow the Lipinski rule of the five [29]. In theory, the oral bioavailability of these compounds will not cause problems, Lipinski's rule has a null violation for both compounds. This suggests that these compounds could be orally favourable and have no permeability issues since they include various groups that act as transporter substrates [30]. According to the Veber rule parameters, [31] compounds that have been tested are flexible molecules because the number of rotatable bonds is less than ten, which indicates that the

molecules are flexible towards their biological targets. Two compounds possessed TPSA values smaller than 140 Å2, indicating that their cell membrane permeability are favorable [32]. In addition, the absorption rate (ABS%) is estimated through the application of the formula ABS% = 109 – (0.345 x TPSA) [33]. It has been noted that, ABS calculated percentage was 73.96%, indicating that these two analogues may have the prerequisite permeability of cell membrane and bioavailability.

Referring to pharmacokinetic and parameters of medicinal chemistry for the compounds **6** and **11** (Table 5), it was established that the two derivatives have high gastrointestinal absorption. Additionally, the ligands are lipophilic and not a substrate of most CYP enzymes. The most important factor affecting absorption is bioavailability, which is a measure of how much drug is present in the plasma. It was demonstrated that two studied compounds had a high degree of bioavailability with score of 0.55. SwissADME [27] achieved Pan Assay Interference Compounds (PAINS), and PAINS-Remover [34] showed zero alerts to the two hits. Scores of the synthetic accessibility for two analogues were determined to be 3.58 and 4.46, respectively. Thus, they can be easily prepared on a large amount.

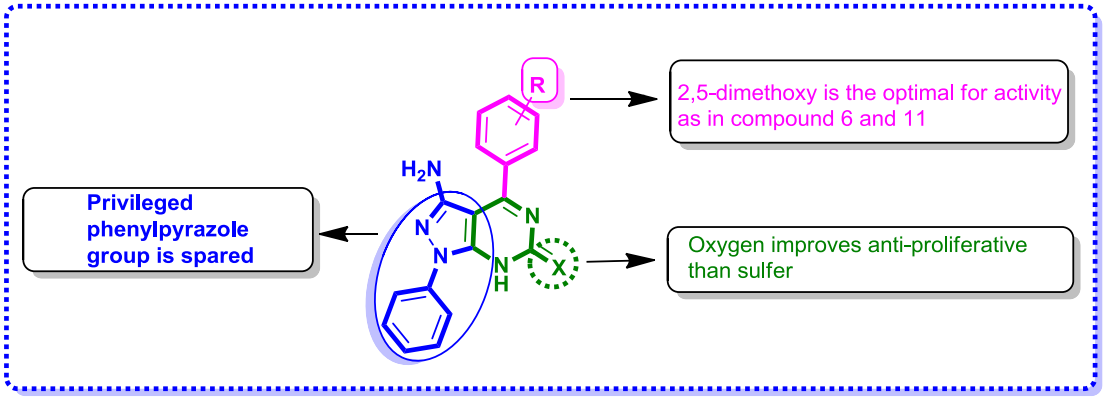

Figure 7. SAR study of pyrazolo[3,4-d] pyrimidines as anticancer agents

4.3.2. Molecular docking study for compounds 6 and 11:

According to docking experimental results, R-roscovitine pose was proved to have identical interactions as documented. In brief, the complex that was docked formed a distinctive H-bond interaction with important active-site residues, such as Leu83 with Roscovitine [C=O with OH (1.59)]. Similarly, the residue Asp86 established hydrogen bond with R-roscovitine's NH (1.97 Å). It showed docking score equal -10.11 Kcal/mol (Figure 4).

Compounds **6** and **11** made good interactions into the active binding region and exhibited favorable connections with the key amino acids. Remarkably, molecule **6** (Figure 5) has two substantial molecular interactions with CDK2's essential amino acid residues. The hydrogen (NH_2) of **6** exhibited a significant hydrogen bond with Leu83 (1.73 Å), in addition to another strong H-bond with Lys 89 via oxygen of OCH_3 (1.65Å) with highest docking score (-10.41 Kcal/mol). Compound **11** (Figure 6), displayed an interaction of Phe 82 with the pyridine ring *via* arene-H interaction. S of C=S presented two

H-bond interactions with Leu83 and Phe82. Another two H-bonds were formed between N of pyrazole ring and hydrogen of NH_2 with Lys89 and Asp86, respectively with docking score (-10.01 Kcal/mol).

5. Conclusion

In conclusion, we have successfully synthesized pyrazolopyrimidine derivatives in high yields. The National Cancer Institute (NCI) tested them for anti-cancer activity. Pyrazolopyrimidines **6** and **11** proved marked cytotoxic effects against glioma cancer cell line (SF-539) with GI values of 85.85% and 63.65%, respectively. Compound **6** showed 1.5-folds the potency of the positive control Roscovitine against CNS cancer subpanels (SF-539) with IC_{50} value 11.1µM. *In silico* analysis found that, the most active derivatives **6** and **11** were in accordance with the parameters of Lipiniski's and Veber's rules. When compared to the ligand Roscovitine, molecular docking of the most potent hits **6** and **11** revealed greater affinities and binding energies to CDK2′s binding site. As a result, compounds **6** and **11** may be considered as promising anticancer candidates.

Supplementary Materials: Appendix A.
Funding: This work is not funded.
Conflicts of Interest: There are no conflicts of interest declared by the authors.
Ethical Statement: NA.

Author Contribution: Author Amel Sabry performed the experimental work and wrote the manuscript. Authors Hend Elsehrawi and Taghreed Shawer supervised the practical work and manuscript writing.

List of Abbreviations: GMB: Glioblastoma multiforme; CDKs: Cyclin-dependent kinases; IR: Infrared spectroscopy**;** NMR: Nuclear Magnetic Resonance Spectroscopy**;** ADME: Absorption, distribution, metabolism, and excretion**;** MW: Molecular weight**;** HBD: Hydrogen bond donor**;** HBA: Hydrogen bond acceptor**;** R. bonds: Rotatable bonds**.**

References

1. Newton HB, Primary brain tumors: review of etiology, diagnosis and treatment. Am. Fam. Physician. 1994; 49: 787-797. [PubMed: 8116514]
2. Davis FG, McCarthy BJ, Current epidemiological trends and surveillance issues in brain tumors. Expert. Rev. Anticancer Ther. 2001; 1:395-401. [PubMed: 12113106]
3. Allam M, Bhavani AKD, Mudiraj A, Ranjan N, Thippana M, Babu PP, Synthesis of pyrazolo[3,4-d] pyrimidin-4(5H)-ones tethered to 1,2,3-triazoles and their evaluation as potential anticancer agents. European Journal of Medicinal Chemistry. 2018; 156:43-52. https://doi.org/ 10.1016/ j.ejmech.2018.06.055
4. Pandey V, Ranjan N, Narne P & Babu PP, Roscovitine effectively enhances antitumor activity of temozolomide in vitro and in vivo mediated by increased autophagy and Caspase-3 dependent apoptosis. Scientific Reports. 2019; 9: 5012. https://doi.org/10. 1038/ s41598-019-41380-1
5. Tripathi D and Imran S, Molecular Docking And In-Silico ADME Studies of Novel Derivative of Erlotinib In Glioma. IJPSR. 2020;11(5):2498-2503.https://www. researchgate.net/publication/341877957
6. Tan AC, MBBS, FRACP, Ashley DM, PhD, MBBS, FRACP, López GY, MD, PhD, Malinzak M, MD, PhD, Friedman HS, MD, Khasraw M, MBChB, MD, FRACP, FRCP, Management of Glioblastoma: State of the Art and Future Directions. CA CANCER J. CLIN. 2020; 70(4): 299-312. doi: 10.3322/caac.21613.
7. Cherukupalli S, Chandrasekaran B, Krystof V, Aleti RR, Sayyad N, Merugu SR, Kushwaha ND, Karpoormath R, Synthesis, anticancer evaluation, and molecular docking studies of some novel 4,6-disubstituted pyrazolo[3,4-d] pyrimidines as cyclin-dependent kinase 2 (CDK2) inhibitors. Bioorganic Chemistry. 2018; 79:46-59.https://doi.org/10.1016/j.bioorg. 2018.02.030
8. Wang J, Yang T, Xu G, Liu H, Ren C, Xie W and Wang M, Cyclin-Dependent Kinase2 Promotes Tumer Proliferation and reduce Radio Resistance in Glioblastoma. Translational Oncology. 2016; 9(6):548-556.http://dx.doi.org/10.1016/j.tranon. 2016. 08.007
9. Husseiny EM, Synthesis, cytotoxicity of some pyrazoles and pyrazolo[1,5-*a*] pyrimidines bearing benzothiazole moiety and investigation of their mechanism of action. Bioorganic Chemistry. 2020; 102:104053
10. Kamel MM, Convenient Synthesis, Characterization, Cytotoxicity and Toxicity of Pyrazole Derivatives. Acta Chim. Slov. 2015;62:136-151.**DOI:**10.17344/acsi. 2014.828
11. Nassar IF, El Farargy AF, Abdelrazek FM, Ismail NSM, Design, synthesis and anticancer evaluation of novel pyrazole, pyrazolo[3,4-d] pyrimidine and their glycoside derivatives. Nucleotides and Nucleic Acids. 2017; 0:1-17. DOI: 10. 1080/15 257770.2016.1276290
12. Cherukupalli S, Chandrasekaran B, Aleti RR, Sayyad N, Hampannavar GA, Merugu SR, Rachamalla HR, Banerjee R, Karpoormath R, Synthesis of 4,6-disubstituted pyrazolo[3,4-d] pyrimidine analogues: Cyclin-dependent kinase 2 (CDK2) inhibition, molecular docking and anticancer evaluation. Journal of Molecular Structure. 2019; 1176:538-551. https:// doi. org/10.1016/j.molstruc.2018.08.104
13. Senderowicz AM, Sausville EA, Pre- clinical and Clinical Development of Cyclin-Dependent Kinase Modulators, *Journal of the National Cancer Institute*, 2000; 92(5): 376-387.
14. Dohm CP, Hülper P, Kermer P, Strik H, Weishaupt JH, Cdk-inhibition as putative new glioblastoma therapy. KlinPadiatr. 2011; 223 -A6, DOI: 10.1055/s-0031-1292587. DOI: 10.1055/s-0031-1292587
15. Nair BC, Vallabhaneni S, Tekmal RR and Vadlamudi RK, Roscovitine confers tumor suppressive effect on therapy-resistant breast tumor cells. Breast Cancer Res. 2011; 13: R80. DOI: 10.1186/bcr2929
16. Pizarro JG, Folch J, Junyent F, Verdaguer E, Auladell C, Beas‐Z arate C, Pallàs M and Camins A, Antiapoptotic effects of roscovitine on camptothecin-induced DNA damage in neuroblastoma cells. Apoptosis. 2011; 16:536-550. DOI: 10.1007/s10495-011-0583-3_

17. Arısan ED, Coker A and Palavan-Ünsal N, Polyamine depletion enhances the roscovitine-induced apoptosis through the activation of mitochondria in HCT116 colon carcinoma cells. Amino Acids. 2012; 42:655-665.DOI:10.1007/s00726-011-1040-x

18. Cho SJ, KimYJ, Surh YJ, Kim BM and Lee SK, Ibulocydine is a novel prodrug Cdk inhibitor that effectively induces apoptosis in hepatocellular carcinoma cells. J. Biol. Chem. 2011; 286: 19662-19671. doi: 10.1074/jbc.M110.209551

19. Liu NA, Jiang H, Ben-Shlomo A, Wawrowsky K, Fan XM, Lin S and Melmed S, Targeting zebrafish and murine pituitary corticotroph tumors with a cyclin-dependent kinase (CDK) inhibitor. Proc Natl Acad Sci.USA. 2011; 108:8414-8419. DOI: 10.1073/pnas.1018091108

20. Coley HM, Safuwan NA, Chivers P, Papacharalbous E, Giannopoulos T, Butler-Manuel S, Madhuri K, Lovell DP and Crook T, The cyclin-dependent kinase inhibitor p57(Kip2) is epigenetically regulated in carboplatin resistance and results in collateral sensitivity to the CDK inhibitor seliciclib in ovarian cancer. Br. J. Cancer. 2012; 106:482-489. doi: 10.1038/bjc.2011.566. Epub 2012 Jan 10

21. Malumbres M and Barbacid M, Cell cycle, CDKs and cancer: A changing paradigm. Nat Rev. Cancer, 2009; 9;153-166. doi: 10.1038/nrc2602

22. Cicenas J, Kalyan K, Sorokinas A, Stankunas E, Levy J, Meskinyte I, Stankevicius V, Kaupinis A, Valius M, Roscovitine in cancer and other diseases. Ann. Transl. Med. 2015; 3:135. DOI: 10.3978/j.issn.2305-5839.2015.03.61

23. Kushwah S, Prajapati K, Darji N, Soni P, Shah P, Synthesis And Pharmacological Screening Of Pyrazolo-pyridine Compounds As Anxiolytices. IJPRBS. 2012; 1:287-315.

24. NCI-60 Screening Methodology, Developmental Therapeutics Program, https://dtp.cancer.gov/discovery development/nci-60/methodology.htm.

25. Mosmann T, Rapid colorimetric assay for cellular growth and survival: application to proliferation and cytotoxicity assays, *J. Immunol. Methods*, 1983;65: 55-63.

26. Abdelsalam EA, Zaghary WA, Amin K M, Abou Taleb NA, Mekawey AAI, Eldehnad WM et al. Synthesis and in vitro anticancer evaluation of some fused indazoles, quinazolines and quinolines as potential EGFR inhibitors, Bioorg. Chem. 2019; 89: 102985.https://doi.org/10.1016/j.bioorg.2019.102985

27. Daina A, Michielin O, Zoete V, Swiss ADME: a free web tool to evaluate pharmacokinetics, drug-likeness and medicinal chemistry friendliness of small molecules. Sci Rep. 2017; 7:42717.

28. Chaudhari PK, Preparation and Biological Evaluation of 3-amino-4-aryl-4,5- dihydro-1-N-tolyl pyrazolo [3,4-d] pyrimidines Derivative. Orient. J. Chem. 2012; 28 (1): 507-512.

29. Lipinski CA, Franco L, Beryl WD, Paul JF, Experimental and computational approaches to estimate solubility and permeability in drug discovery and development settings. Advanced Drug Delivery Reviews. 2012; 64:4-17. https://doi.org/10.1016/S0169-409X(00) 00129-0

30. Kitchen DB, Decornez H, Furr JR, & Bajorath J, Docking and scoring in virtual screening for drug discovery: Methods and applications. Nature Reviews. Drug Discovery. 2004; 3(11):935-949. https:// doi.org/10.1038/nrd1549

31. Veber DF, Johnson SR, Cheng H-Y, Smith BR, Ward KW, Kopplem KD, Molecular properties that influence the oral bioavailability of drug candidates. J. Med. Chem. 2002; 45:2615.

32. Wang JL, Li L, Hu MB , Wu B, Fan WX, Peng W, Wei DN, & Wu CJ, In silico drug design of inhibitor of nuclear factor kappa B kinase subunit beta inhibitors from 2-acylamino-3-aminothienopyridines based on quantitative structure-activity relationships and molecular docking. Computational Biology and Chemistry. 2019;78:297-305.https://doi.org/ 10.1016/j. compbiolchem.2018.12.021

33. Zhao YH , Abraham MH , Le J, Hersey A, Luscombe CN , Beck G , Sherborne B, and Cooper I . Rate-Limited Steps of Human Oral Absorption and QSAR Studies. Pharmacol. Res. 2002; 19 (10): 1446-1457.

34. Jonathan BB, Georgina AH, New substructure filters for removal of pan assay interference compounds (PAINS) from screening libraries and for their exclusion in bioassays. J. Med. Chem. 2010; 53:2719-2740. https://doi.org/10.1021/jm901137j